A new VTOL propelled wing for flying cars: critical bibliographic analysis

TRANCOSSI, Michele <http://orcid.org/0000-0002-7916-6278>, HUSSAIN, Mohammad, SHIVESH, Sharma and PASCOA, J

A new VTOL propelled wing for flying cars: critical bibliographic analysis

Author, co-author (Do NOT enter this information. It will be pulled from participant tab in MyTechZone)

Affiliation (Do NOT enter this information. It will be pulled from participant tab in MyTechZone)

Abstract

This paper is a preliminary step in the direction of the definition of a radically new wing concept that has been conceived to maximize the lift even at low speeds. It is expected to equip new aerial vehicle concepts that aim to compete against helicopters and tilt rotors. They aim achieving very good performance at very low speed (5 to 30 m /s) by mean of an innovative concept of morphing ducted-fan propelled wing that has been designed to maximize the lift force. This paper presents an effective bibliographic analysis of the problem that is a preliminary necessary step in the direction of the preliminary design of the wing. A preliminary CFD evaluation allows demonstrating that the claimed results are in line with the initial expectations. According to the CFD, results it has been produced a preliminary energetic evaluation of the vehicle in a flying car configuration by EMIPS method. Even if the results are still preliminary, they allow evidencing a good energy efficiency of the vehicle against helicopters.

Introduction

Generalities

This paper presents a radically new wing design that aims to equip radically new aircraft designs such as flying car or other new aircraft architectures with the aim of emulating the behaviour of helicopters and tilt rotors with much higher efficiency, better performances and higher safety levels. The specific design has been realized to allow producing typical manoeuvres including VTOL operations and hovering by mean of a radically new and simple high-chamber morphing wing with an embedded ducted fan. It has a dual configuration: the first one aims to increase lift by mean of Coandă effect [1] and super circulation [2] and the other one aims to produce a vertical thrust by jet deviation. It is derived by a family of possible configurations, which have been preliminarily originated by the optimization of the energy balance of a helicopter in flight. By optimizing this model, it is possible to define a new vehicle concept that can do anything that a helicopter can do with mayor energetic benefits. The above analysis identifies the possibility of overcoming the energetic limits of rotary wing aircrafts with respect to other vehicles [3]. In particular, the future environmental exigencies of greening aeronautics have focused the attention on possible solutions that can be electrically propelled [4-7]. The main characteristics ore the proposed wing design are the following.

1. distributed electrical propulsion by mean of ducted fan propellers embedded into the wing [11, 12];
2. acceleration of the fluid stream on the upper surface of the wing by mean of EDF propellers [13] that produces a much higher lift coefficient, with respect to any other aircrafts (up to 9-10);
3. very low stall speed (lower than 10m/s) and consequent increase of the flight envelope in the low speed domain up to 10÷12 m/s;
4. flight at lower velocity than stall speed by the innovative flaps that can change both the configuration of the aircraft in flight and the direction of the thrust by mean of Coandă effect [14].

The functional scheme shows clearly the two configurations of the wing. It can assume a position that produces an increased lift force by mean of the coupled action of both Coanda effect on the convex surface of the mobile wing and the attraction effect on the high-speed stream. This configuration is adequate for high-speed cruise flight. A second configuration is obtained by mean of an axial rotation of the rear wing for low speed flight to produce an almost vertical direction of the thrust. with an almost vertical lift coefficient and more deflected thrust, and by mean of fluid deflection to an almost vertical direction of thrust for vertical take off and landing (VTOL) and hovering [15].

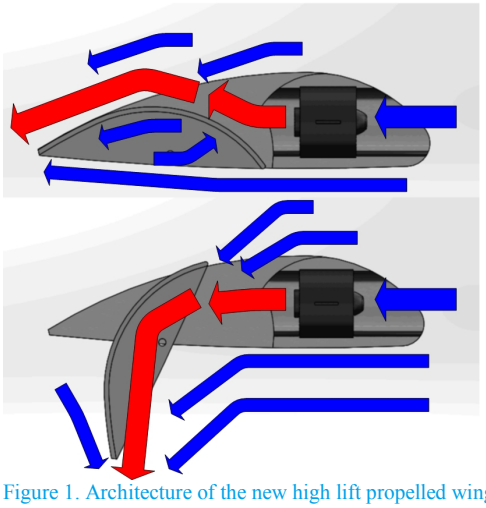

Figure 1. Architecture of the new high lift propelled wing.

Simplified energy balance of air vehicles

With the development of aviation technology, helicopter has coupled effective performances and flexibility [16-17] with lower energy efficiency with respect to any other vehicle [18]. The energy inefficiency of helicopters has been demonstrated specifically by Trancossi who has performed an effective comparison of the

energetic performances of different vehicles by EMIPS (Exergetic Material Input per Unit of Service) [19, 20] method.

Trancossi [11] has modified the former assessment method by Dewulf by considering the mass of the vehicle (whatever is his nature) divided into the mass of the vehicle and the mass of the payload. In this way, he analyses the energy efficiency of the vehicle and the one for moving the payload. The results for helicopters have identified their energetic and exergetic inefficiency.

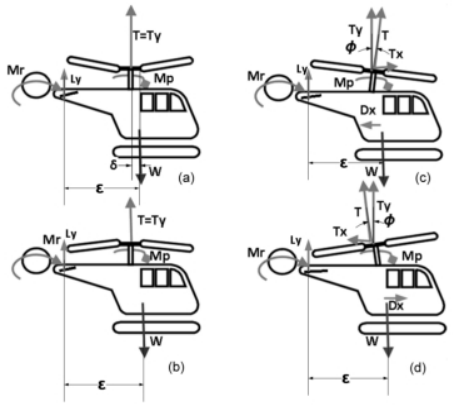

Figure 2. Forces on a helicopter during flight.

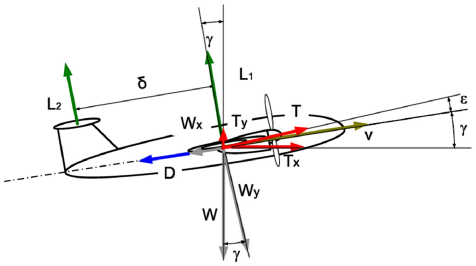

Figure 3 Forces on an aircraft during flight.

Helicopter are capable of vertical take off and landing, vertical movements, forward and reverse flight, and hovering. Having a very limited aerodynamic lift, they need a much higher thrust also in vertical direction. The forces that apply to helicopter during different flight conditions are summarily presented into Figure 1. The forces applied on a helicopter changes in different flight conditions [22] and the equations of flight mechanics of helicopters can be obtained from Phillis and Venkatesan [23].

$$\begin{cases} ma_x = T\sin\phi - D_x \\ ma_y = T\cos\phi + L_y - W - D_y \\ I\dot{\omega}_z = \delta \cdot T \cdot \cos\phi + \varepsilon \cdot L_y \\ M_p + M_r = 0 \end{cases} \quad (1)$$

Three different conditions can be evidenced: vertical flight (Figure 1.a and b) forward flight (Figure 1.c) and reverse flight (Figure 1.d).

According to figure 2, it is possible to express the equations of flight of an aircraft [24, 25] that can apply also to tilt rotors in horizontal flight.

$$\begin{cases} ma_x = T\cdot\cos(\gamma+\varepsilon) - (L_1+L_2)\cdot\sin\gamma - D\cdot\cos\gamma \\ ma_y = T\cdot\sin(\gamma+\varepsilon) + (L_1+L_2)\cdot\cos\gamma - W - D\cdot\sin\gamma \\ I_z\dot{\omega}_z = \delta\cdot L_2 \end{cases} \quad (2)$$

In horizontal flight they become

$$\begin{cases} ma_x = T\cdot\cos\varepsilon - D \\ ma_y = T\cdot\sin\varepsilon + L_1 + L_2 - W \\ I_z\dot{\omega}_z = \delta\cdot L_2 \end{cases} \quad (2')$$

Wood [9] and Zuang [26] have developed helicopters energetic flight models of a helicopter. From it can be possible to derive the equation of the energy state of a generic multicopter with *n* propellers at any altitude airspeed-RPM combination:

$$E = \frac{1}{2}mV^2 + mgh + \sum_{i=1}^{n}\frac{1}{2}I_i\Omega_i^2 \quad (3)$$

Equations (2), (2') and (3) can describe also tilt rotor aircrafts, such as Boeing Osprey, which allow coupling some of the features of helicopter and some of the features of aircraft.

Tiltrotors

Tilt rotors are aircrafts, which can tilt their propellers allowing them to operate with vertical (helicopter mode) or horizontal axis (airplane mode). Military users use Tilt rotors, even if some civil vehicles are going to be delivered on the market.

Tilt rotors, such as Boeing Osprey [27], have large tilting propellers that can assume both vertical axis (helicopter mode) and horizontal axis (airplane mode). They are mostly used in military field, but some civil concepts have been presented. They have problems and operative limits [28]: vibrations of drive shafts, coupled wing/shaft flexing, high disc loading generates excessive downwash, instability when wing angle is between 35° and 80°.

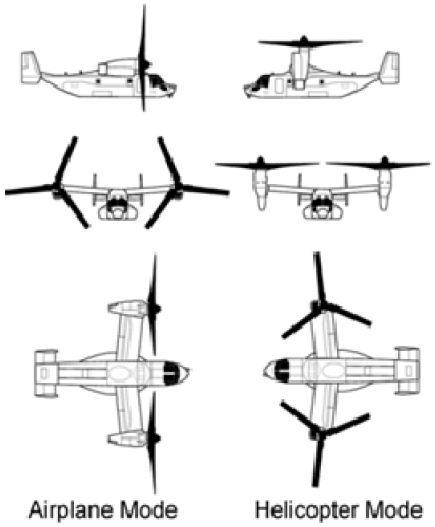

Figure 4: Tilt rotor aircraft configurations during flight

They have also a lower efficiency against helicopters in vertical flight and against aircraft in horizontal flight [29]. In particular, the Phase II

report on Osprey [29] demonstrates that a twin-engine commercial tiltrotor derived from the military V-22 would be comparable to a medium-size commuter turboprop and could carry around 40 passengers up to 600 miles. It would be capable of vertical takeoff and landing, but short takeoff and landing rolls would improve payload or range. Tiltrotors could use existing airports, but 40-seat versions would be too large for many heliports. To compete with airline shuttle service, passenger cabin noise, vibration, and overall comfort levels will have to be at least equivalent to that of commuter aircraft, such as the DeHavilland Dash 8-300. Compared with turboprop aircraft, a tiltrotor would cost around 40 to 45 % more to produce and about 14 to 18 % more to operate (over a 200-mile trip).

In addition, they have suffered of some operative problems [30] since vertical landings at unimproved sites produce massive dust clouds that are ingested into its engines. This is why V-22s rarely stray from hard surface runways, and prefer rolling take-offs to outrun any dust. This particular problem forced to introduce limits in operations.

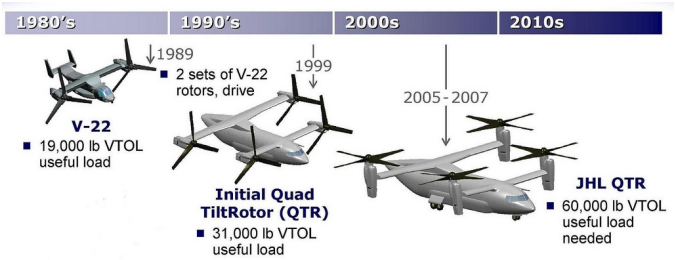

Figure 5. Expected development of tilt rotors

Autogyros

Autogyros [31, 32] have a horizontal axis propeller and a free-spinning rotor actuated by the relative motion in air that sustains the autogiro [33]. Autogyros had a large success both in civil and military aviation. Development continued to bring the rotor up to a sufficient speed for takeoff. The Pitcairn-Cierva Autogiro solved the problem with a mechanical power transmission, which can be detached by a clutch.

Figure 6 De la Cierva 1923 autogyro.

A particular architecture of autogiros is Rotodyne [34]. It was a 1950s compound gyroplane realized by Fairey Aviation for both commercial and military applications [32]. The Rotodyne has been conceived as autogyro design propelled by coupled tip jet-powered rotor that burned a mixture of fuel and compressed air produced by two wing-mounted turboprops. The rotor has been powered during VTOL operations, hovering and low-speed translational flight. It was autorotating during cruise flight in which the necessary power has been produced by to two propellers applied to the turboprops. The project was stopped because of huge acoustic problems.

Figure 7 Fairey Rotodyne

Propelled wings

Another competitor of helicopter is propelled wing architecture. Propelled wings have been designed with multiple concepts that can couple also with diffused propulsion concepts:

1. *Magnus Effect enhancers* introduces cylinders propeller into a wing increasing fluid adhesion [35].

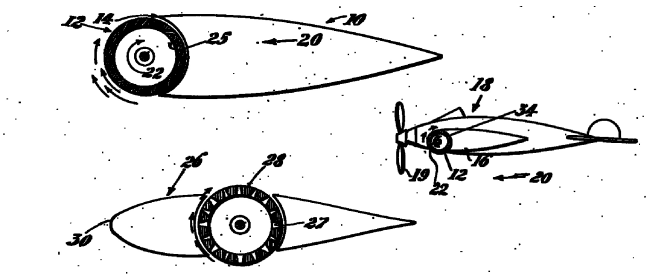

Figure 8. Magnus effect enhancer or propulsion (1941)

2. *Jet diffusers* [36, 37] couple jet propulsion with wings. Jet wing discharge distributes the jet exhausts using channels inside the wings and coupled with mobile flaps that allow orienting the jet (Figure 1). Wing-mounted jet-propulsion system [38] develops a similar concept, by mean of multiple jets inside a wing.

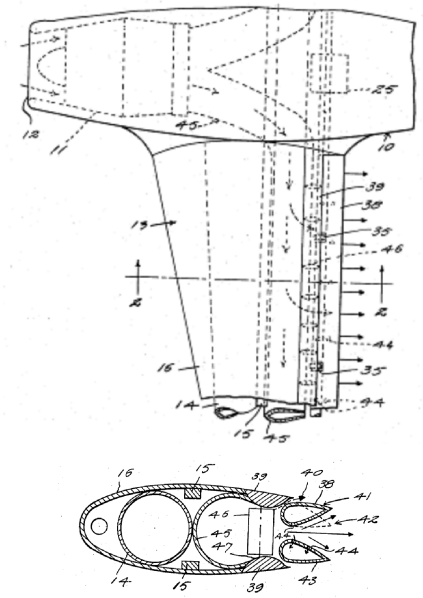

Figure 9. Jet wing discharge propulsion system (1949)

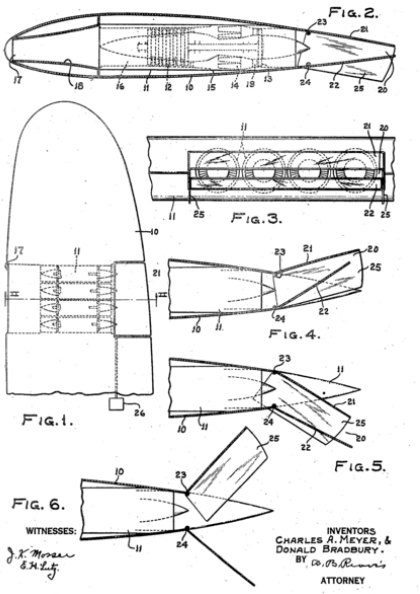

Figure 10. Wing mounted jet propulsion

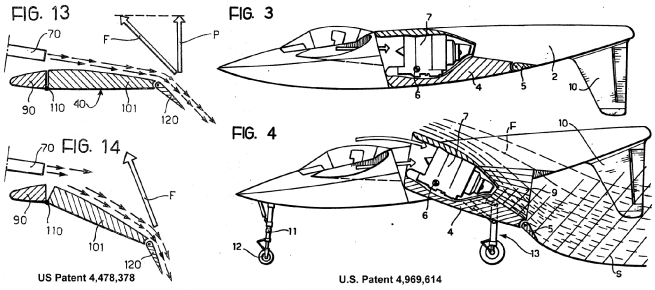

Figure 11. The patents by Capuani

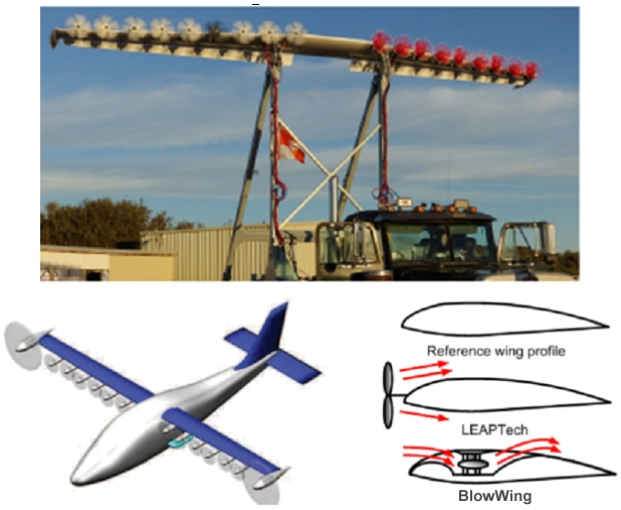

Figure 12. LEAPTech wing mounted on the testing truck during ground test activities; NASA SCEPTOR 3D models; comparison between LEAPTech the much higher lift generated by the present propelled wing concept.

Coandă effect enhanced aircrafts

Capuani [39, 40] has proposed a jet-propelled aircraft in which propulsion jets are directed over the top surface of the wing (Figure 11). It produces additional lift because of the supercirculation induced on the wing and the deflection of the jets downwards by mean of Coandă effect, immediately downstream of the wing is provided with two longitudinal surfaces projecting from said top surface to form a single surface ejector system.

The results of the former EU FP7 ACHEON (Aerial Coandă High Efficiency Orienting Nozzle) Project [41, 42] has demonstrated that it is possible to produce a propulsive synthetic jet, which is generated by two impinging streams, by mean of Coandă effect (Fig.1). The core of the ACHEON thrust and vector propulsion is a nozzle with two internal channels, which converge in a single outlet with two facing Coandă surfaces (3) and (3').

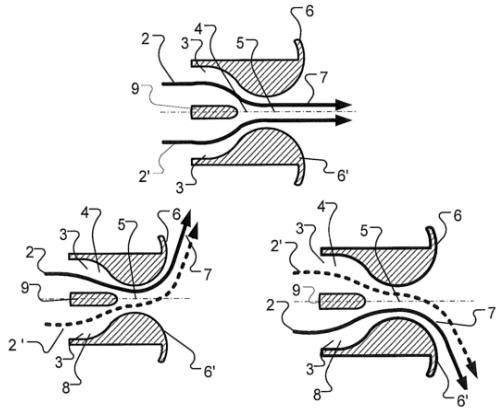

Figure 13. ACHEON Nozzle concept

Two impinging jets (2) and (2') generate a synthetic jet that proceeds straight if the streams have equal momentum, or adheres to the Coandă surface on the side of the stream with higher momentum. Control and stability are increased by Dielectric Barrier Discharge (DBD) installation [43, 44]. In particular, DBD has been experimented during the project into two different functions:

1. increasing the adhesion with a DBD jet directed in the direction of the fluid stream;
2. Reducing the rigidity and favouring the detachment by mean of a contrary jet.

The architecture fits with electric propulsion and subsonic aircrafts (Mach 0-0.5). In particular, it has verified that the deflection angle of the jet (and of the thrust) is a function of both momentums (and speeds) of the two primitive streams and the geometric configuration of the nozzle [45, 46]. Trancossi et al. [47, 48] have clearly demonstrated the advantages of ACHEON in case of application to STOL aircraft in terms of takeoff roll and in case of horizontal flight.

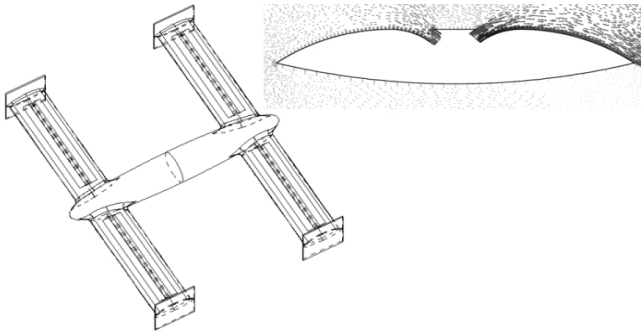

Figure 14. Preliminary conceptual design of the aircraft [30]

Interesting fallout of the ACHEON project has been the preliminary concept of a new propelled wing configuration [3] and produced an

effective energy model of a drone based on that wing (Fig. 2). The key advantage of this configuration is an almost perfect emulation of the behaviour of helicopters by a reversible system. This solution can be interesting but it is still under development. It require effective ducted system from inlet to the compressor and then to the outlet with reasonable pressure losses. Another hypothesis is a reversible propeller/compressor for propulsion that can be hosted inside the wing and ensure minimum pressure losses.

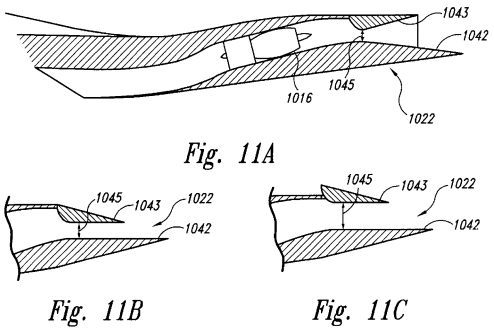

Figure 15. Nelson's propulsion nozzle

Nelson has studied a new aircraft modular design, with a propulsion system, including an engine, inlet, and exhaust nozzle can be integrated into the aft body to be at least partially hidden behind the wing [49]. In one embodiment, the entrance of the inlet can be positioned beneath the wing, and the exit of the nozzle can be positioned at or above the wing.

Radelspiel [50] has developed an important variable geometry wing jet discharge concept that uses tangential blowing of thin wall jets to overcome the adverse pressure gradients from locally very large flow turning rates increasing the Coandă effect. It also uses oblique blowing of air jets to generate longitudinal vortices in the boundary layer and to provide a convective redistribution of momentum in the boundary layer with an increase of turbulent momentum transport. Radelspiel has also produced an important activity on the influence of stream-wise vortices on a generic high-lift configuration [51].

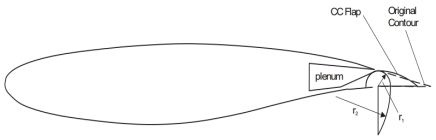

Figure 16. Radelspiel's dual curvature flapped wing [31].

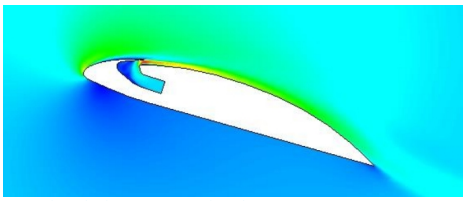
Figure 17. Supercirculation rotary wing by Drăgan

It is also important to cite the huge activity produced on the efficiency of turbo-machineries by Drăgan [52] who has coupled traditional theoretical research with CFD. In particular, Drăgan has assessed the robustness of the models of Coandă effect by Roderick [53] and Benner [54]. Drăgan [55] has also produced a fundamental reference regarding coupling super circulation with Coandă effect adhesion on rotary wing propulsion.


Figure. 18. NASA LEAPtech wing during tests (NASA Web site).

Some attempts of increasing the lift are connected to diffused propulsion embedded into the trailing of the wing. The most successful sample in this direction is constituted by the NASA LEAPtech project [56]. The project is indented to increase the lift coefficient of an aircraft wing by mean of diffused electric propulsion. During preliminary testing on board of a truck, lift coefficients CL in the range 5 - 7 have been achieved (Figure 4).

The integration of a LEAPTech wing into an aircraft will produce NASA's SCEPTOR project [58], which will convert a Tecnam into the X-57. It aim to improve the aerodynamic efficiency in cruise by reaching a better positioning of the cruise point along the drag polar, reducing the wetted area and increasing the aspect ratio of the wing [59]. Multiple propellers along the leading edge increases the local Reynolds number and produce some increase in term of friction drag together with some disturbances in the lift distribution over the wing.

Theoretical background

A new propelled wing concept

The proposed propelled wing concept has been inspired by Nelson's nozzle [49], and the studies by Benner [54], Drăgan [52] and Trancossi's blowing wing concept [3]. It is based on a dual system based on an unconventional high lift wing coupled with an electric ducted fan unit blowing on the top surface of the wing (Fig. 5).

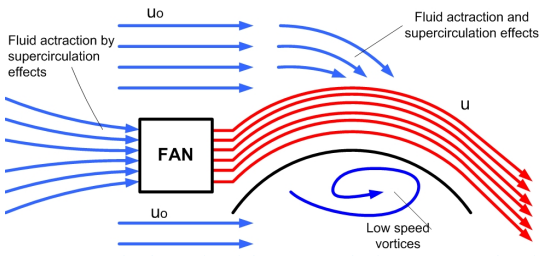

Figure 19. Conceptual schematic of the proposed wing concept (showing in red) expected effect of Coandă adhesion

Using Benner's model it can be possible to describe Coandă adhesion in terms of equilibrium between centrifugal and pressure forces:

$$F_c = \frac{\rho \cdot R \cdot d\theta \cdot dRu^2}{R} \quad (4)$$

$$F_p = R \cdot d\theta \cdot dp \quad (5)$$

where, $d\theta$ is the infinitesimal angular element.

The model of the system can be subdivided into two control volumes according to Fig. 6. The first one is dominated by fluid deviation by

means of the presence of the interaction of the jet through a surface. The second one is dominated by the Coandă adhesion caused the pressure phenomena.

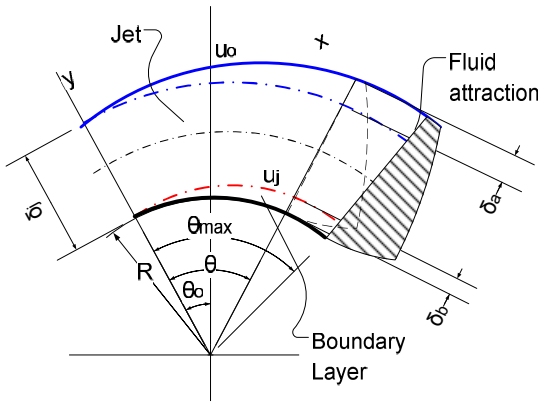

Figure. 20. Structure of the fluid dynamic jet

Pressure drop along the jet can be expressed according to Benner [54] who present a crude but functional model for h/R ratios smaller than one. He produces a balance between the pressure forces and the centrifugal forces acting upon a volume of fluid.

$$y: \quad p_{static\,jet} - p_{atm} = -\frac{\rho \cdot u^2 \cdot h}{R} \qquad (6)$$

Benner equation is based on difference on pressure only and works properly only for the condition h/R<1 and does not consider the shear stress and the external fluid attraction. Dragan has verified the robustness of this formulation, but has also evidenced the necessity of introducing a correction to allow Benner equation to fit better numerical results. This activity on Benner model integrates with the models by Trancossi [45,46]. The aim is not the production of any corrective coefficient that can fit the results, but the definition of a robust theoretical model that can fit a set of problems that have been marginally studied. In particular, the proposed area of interest focus in a large jet that blows almost tangentially on a convex surface. This preliminary definition of a new wing concept assumes that R is large some considerations can be done about the fluid jet development and it can be considered that the development of the boundary layer is similar to the one over a flat plate. In particular, it can be assumed that the thickness δ of the jet is given to two different thicknesses: δb that refers to the boundary layer being caused by shear stress and to δa that refers to the jet and is caused by the phenomena of fluid attraction from the surrounding free stream.

Considering a preliminary 2D model the following assumptions can be adopted:

3. The length over the Coandă surface has been indicated with x, $x = R\theta$
   where θ is the generic angle of contact.
4. The Coandă jet considering the effects involved has been considered as the combination of three effects:
   a. the boundary layer effect governed by shear stress;
   b. the equilibrium of centrifugal and pressure forces (main Coandă effect);
   c. the attraction of the surrounding slower fluid;
5. The three effects can be considered separately and their effects can be added by superposition. In the core zone of the fluid, over the boundary layer boundary, the velocity is kept at least in one point equal to the initial velocity of the jet;
6. The jet has an initial constant profile of velocity.

The gauge pressure at the nozzle outlet is zero (i.e., $p_2 = 0$), since air is discharged to the atmosphere. According to the principle of conservation of mass, neglecting the fluid attraction phenomena, it results:

$$A_{jet} \cdot u_{jet} = A \cdot u \rightarrow u = \frac{A_{jet}}{A} \cdot u_{jet} \quad (4)$$

By assuming $x = \theta \cdot R$, and assuming, that R is sufficiently large, it has preliminary modeled the boundary layer according to the model which is used for the boundary layer on a flat plane. For the boundary layer term it can be possible to consider the solution by Schlichting [70] in a turbulent regime:

$$\mathrm{Re}_x = \frac{\rho \cdot u \cdot x}{\mu} \rightarrow \delta_b = 0.37 \frac{x}{\sqrt{\mathrm{Re}_x}} \quad (5)$$

$$\mathrm{Re}_x = \frac{\rho \cdot u \cdot x}{\mu} = \frac{\rho \cdot u \cdot \theta \cdot R}{\mu} = \theta \cdot \mathrm{Re}_R \quad (6)$$

Skin friction for turbulent flows is given by

$$C_f = \frac{0.0594}{\mathrm{Re}_x^{0.2}} = \frac{0.0594}{(\theta \cdot \mathrm{Re}_R)^{0.2}} \quad (7)$$

Wall shear stress is another parameter of interest in boundary layers. It is usually expressed as a function of skin friction defined as:

$$C_f = \frac{2\tau}{\rho \cdot u^2} \rightarrow \tau = \frac{1}{2} C_f \rho \cdot u^2 = \frac{1}{2} \cdot \frac{0.0594}{(\theta \cdot \mathrm{Re}_R)^{0.2}} \mathrm{Re}_R^2 \frac{\mu^2}{\rho \cdot R^2} \quad (8)$$

and

$$\delta_b = 0.37 \frac{x}{\sqrt{\mathrm{Re}_x}} \cong 0.37 \cdot (\theta \cdot \mathrm{Re}_R)^{0.5} \cdot \frac{\mu}{\rho \cdot u} \quad (9)$$

The fluid attraction phenomena can be modeled by the interaction of the external fluid and the jet. It is consequent of the difference between the static pressures of the surrounding fluid and the Coandă jet. It generates a reduction of the average velocity of the fluid, but generates an effective augmentation of the mass flow. This phenomenon presents more difficulties in term of an effective modeling. It has been preliminarily neglected.

Preliminary evaluation of the concept

A coupled study of both helicopters' flight mechanics and of the above-cited theoretical and conceptual references has allowed synthesizing a radically new morphing wing concept according to the operative schema described in Figure 19. It is composed by a front propulsive section and a rear bi-sided mobile convex/concave high camber and low thickness wing profile (Figure 13). It has a dual mode configuration. It increases the lift when the propulsive fluid stream flows over the convex wing profile by coupled action of high speed on the top surface and attraction on the surrounding fluid. It generates a vertical thrust by fluid deviation on the concave surface of the wing during takeoff, landing, hovering and very low speed operations.

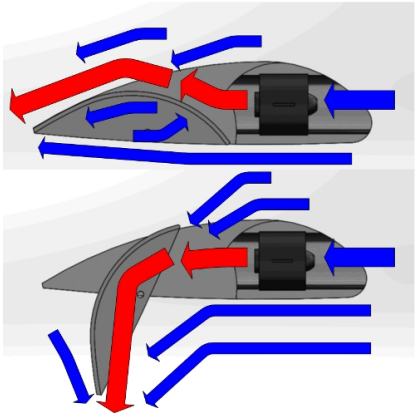

Figure 21 - Architecture of the high lift propelled wing.

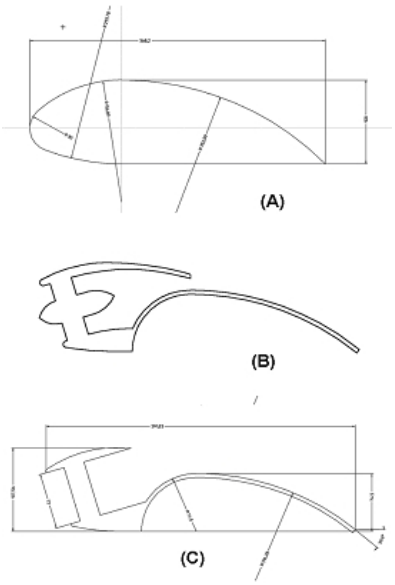

Figure 22. Preliminary wing design: (A) reference wing, (B) initial wing design; (C) final modified design

CFD setup method

Ansys Fluent 17.1 has been used for preliminary CFD simulations. They have been performed according to ERCOFTAC guideline [59] as described by Rizzi [60] and Celik [61], and by referencing Dragan [55], Schlichting [62], Pfingsten [63], and Besagni [64]. The numerical stability of the grid has been verified in unsteady conditions through the numerical computation of the grid at different refinement levels. It has been found that, when the grid resolved the viscous sub-layer until y+ value less than 2, it is possible to get the jet deflection angle independent of the grid. Two different turbulence models have been used Spalart Allmaras [65, 66] for preliminary setup and SST K-ω [67, 68] model. Second order upwind scheme has been used to discretize the momentum equation and of k and ω model. Pressure and velocity have been coupled through the PISO (Pressure-Implicit with Splitting of Operators) method [69]. Pressure gradient term has been discretized using PRESTO (PREssure STaggering Option) method [70]. The PRESTO scheme provides improved pressure interpolation in situations where large body forces or strong pressure variation are present. Unsteady term has been discretized using first order implicit method [71] taking advantage of unconditionally stable with respect to time step size, which has assumed $\Delta t = 1 \times 10\text{-}03$ s.

Preliminary cfd activity

The design has been preliminary verified by mean of preliminary 2D CFD simulations. A preliminary CFD investigation on a 2D model has been performed in order to produce a preliminary optimization of the shape.

The study considers an initial design (Figure 14) which is based on a high-thickness wing profile that can reach high-lift values. .

The preliminary wing shape (Figure 22/A) has been initially modified host a propeller and a second section that can move assuming different positions (Figure 22/B). Both 2D and 3D simulations have been performed. Final meshes have been generated assuming the following parameters:

1. lines discretization: 2.5 10^{-3} m;
2. inflation layers: height: 0.25 10^{-3}; expansion factor: 1.1; total levels: 10; max aspect ratio: 1/5.

A sample of the mesh of the wing is provided in figure 23. In particular, the following parameters have been reached: max skewness: 1.54, max aspect ratio: 9.11.

Those preliminary results have produced a huge modification in the system architecture with the objective of reducing the pressure losses. From this very preliminary CFD it has been possible to produce a new architecture (Figure 22/C) with deep modifications in the propeller area, which has been deeply analyzed by 2D simulations (Figure 24).

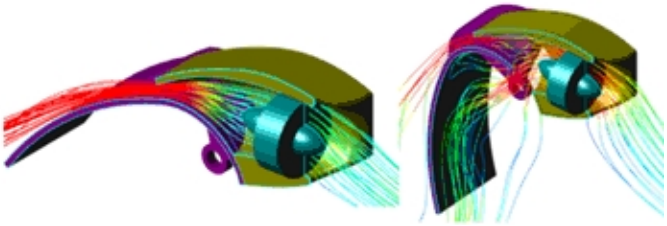

Figure 23 - Preliminary configuration 3D CFD

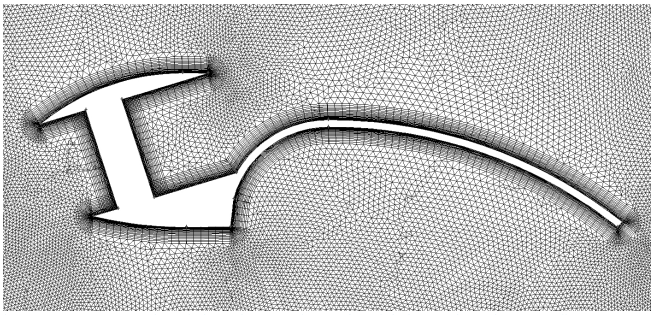

Figure 24 - Example of the Fluent tri-mesh with boundary layer refinement

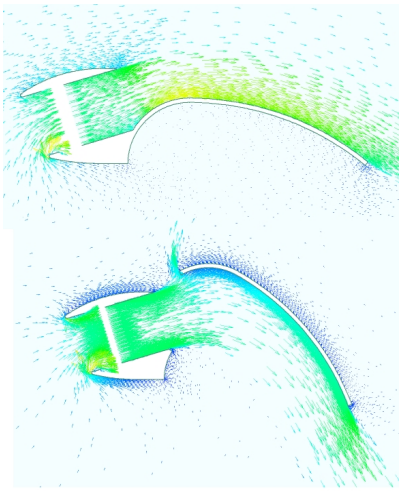

Figure 25 - An example of CFD solution

The simulations have been performed at different airspeeds in the range U_o=*0÷20 m/s* and different jet speeds U_j=*Uo+5÷Uo+30 m/s*.

Different cases have been evaluated. The reference wing has been simulated in the same range.

Results have been reported for the configuration in Figure 22/C. Sample velocity vectors has been presented in Figure 25. The results have been analytically reported:

1. lift and drag for the reference wing in Figure 18,
2. lift for the propelled wing profile in Figure 19,
3. drag and lift coefficients in Figure 28 and 29.

It can be observed that CD and CL appear specifically variable and dependent on the intensity of the Coandă Jet.

The front air intake has the advantage of allowing an effective reduction of Drag by mean of the front air intake. The results show clearly the expected lift and drag results.

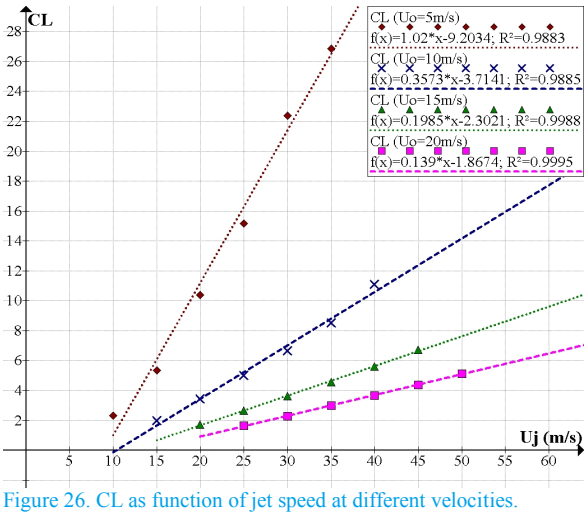

Figure 26. CL as function of jet speed at different velocities.

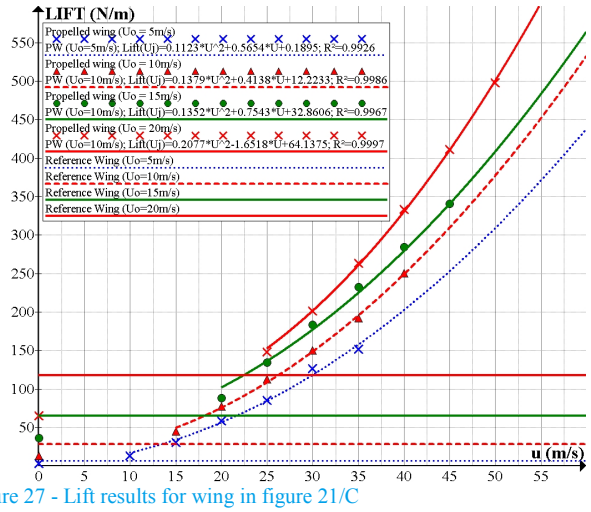

Figure 27 - Lift results for wing in figure 21/C

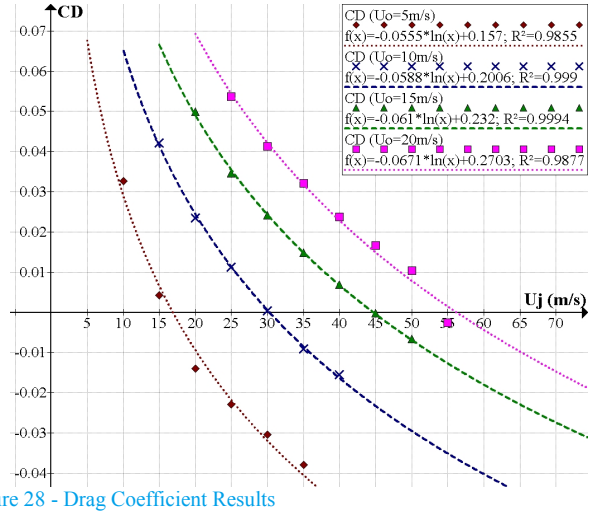

Figure 28 - Drag Coefficient Results

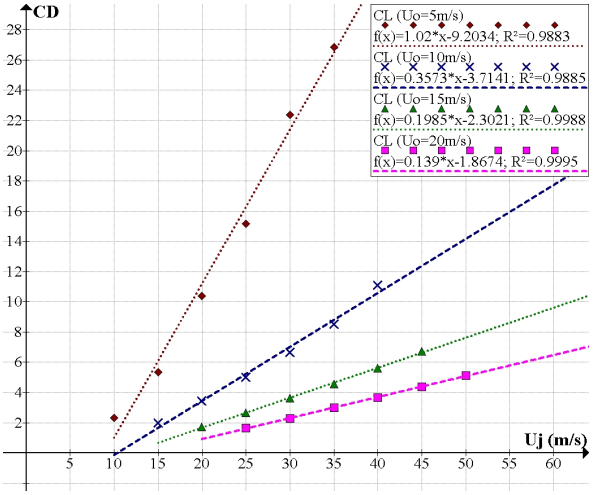

Figure 29 - CL as function of jet speed at different velocities.

Figure 29 shows clearly that the it is possible to notice the main problem, which has been identified and regards explicitly the interaction between the high speed stream and the mobile high chamber wing profile that has been installed. The optimization of the mobile wing profile has been considered fundamental for producing a more effective wing profile.

Analysis of CFD results

The results appear to be clearly in line with the Coanda effect models, which have been presented by Roderick and Brenner. In fact, it is evident the correlation between the angle of attachment and the geometric parameters of the Coanda surface. This preliminary theoretical evaluation of the results is being currently analysed according to first and second law.

On the other side, the results allow to define the redesign of the wing system to correct the defects and improve the limits of the tested configuration. The redesign activity has been focused on reducing internal pressure drops caused by the reduction of the exit section and on a better shaping and kinematic analysis of the moving wing to improve the fluiddynamic behaviour when the wing is used to produce vertical thrust. A preliminary result of the redesign activity has shown in Figure 30. This new configuration is currently under massive CFD testing with the objective of producing a more effective design that improves radically actual design.

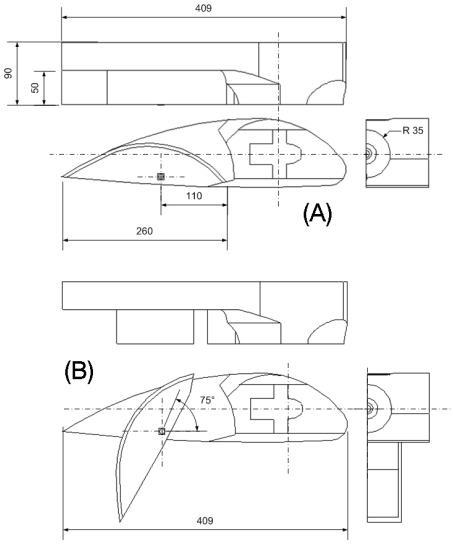

Figure 30 - **Main measures of the wing**

Flying cars

This vehicle can insert into the segment of the flying cars. Major competitors appear to be a vehicle, which is currently far from any optimization and appears like cars with deployable wings. Most of them are not VTOL and must take off from airports. They do not present any real operative advantage with respect to an aircraft.

1. *AeroMobil* is a car with deployable wings. It is under testing in ultra-light category (Czech certification). When the final product will be available or how much it will cost is not specified. [72]

Figure 31. Aeromobil flying car

2. *Urban Aeronautics' X-Hawk* and Airmule (unmanned) is a VTOL turbojet [73] powered aircraft announced in 2006 with a first flight planned for 2009. It was intended to operate like a tandem rotor helicopter, with ducted fans rather than exposed rotors. As of 2015, no flights had been reported.

Figure 32. Xplorair AirMule prototype and XHawk drawing

3. Moller Skycar M400 [74, 75] is a personal VTOL (vertical take-off and landing) aircraft that act as a tilt rotor with four pairs of ducted fan propeller moved by Wankel rotary engines.

Figure 33. Moller Skycar prototype

Skycar would be allowed to fly from airports & heliports. They have proposed an all-electric version.

4. The Xplorair PX200 [76] is a project of single-seater VTOL aircraft without rotating airfoil, relying on Coandă effect and using an array of small jet engines called "thermoreactors" embedded within tilt wings' body. A full-scale drone has scheduled for flight at Paris Air Show 2017.

Figure 34. Xplorair PX200

5. Terrafugia TF-X [77] is an electric hybrid tilt-rotor vehicle that would be the first fully autonomous flying car. It has a range of 500 miles (800 km) per flight and batteries are rechargeable by

the engine. Development of TF-X is expected to last 8–12 years (2021–2025).

Figure 35. Terrafugia TF-X

6. Macro SkyRider X2R [78] is a project of a flying car which is lighter than the Moller Skycar.

Figure 36. Macro SkyRider X2R

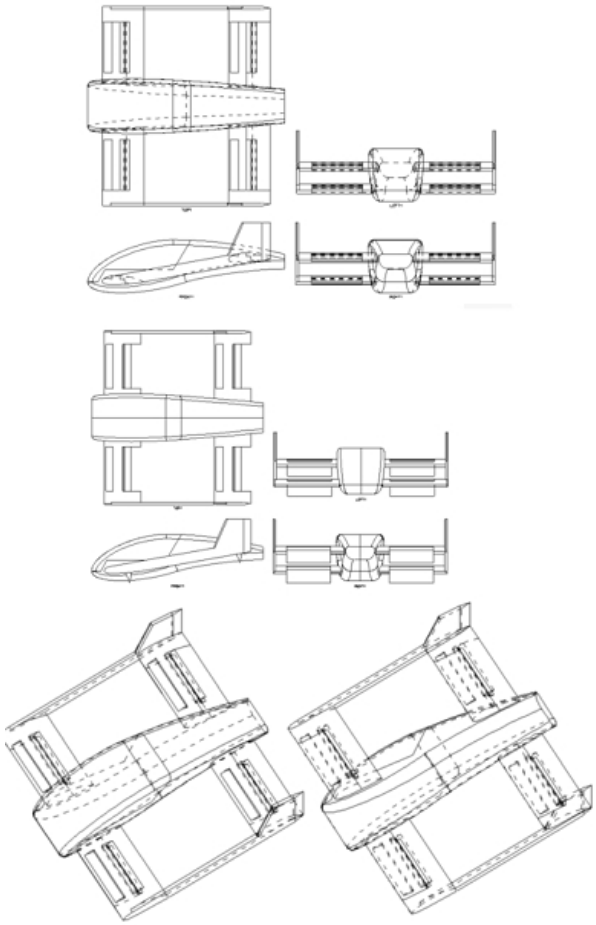

Figure 37. Preliminary aircraft architecture

Preliminary vehicle definition

The proposed wing is expected to be the key component of a novel urban all-electric flying vehicle. It is a two-seater (FAA-EASA Light-Sport aircraft) with a MTOW lower than 600 kg and a price in line with high-class cars (around 90,000 €). The dimensions (length and wingspan lower than 7 m) allow operations from large urban roads for personal transport, emergency, civil protection and police use. It has the objective of substituting or integrating ground transport and helicopters. It has an exceptional operative flexibility by performing both VTOL and STOL operations. It can be defined by using industrial grade battery (the BASF Ovonic NiMH battery that was installed on the GM EV-1 [79]) with 80 Wh/kg at the cell level, and a power discharge of 100 W/l.

Figure 38. An emotional rendering.

By assuming the preliminary results produced by Hussain [80] and and Trancossi [81] in terms of performance of the wing it is possible to produce a vehicle assessment that demonstrate the potential of the proposed vehicle. In the case of this electric vehicle, because of the necessity of comparing solution with different fuels and propulsion systems, GHG are evaluated at the 2014 value of EU GHG emission factor for electric production.

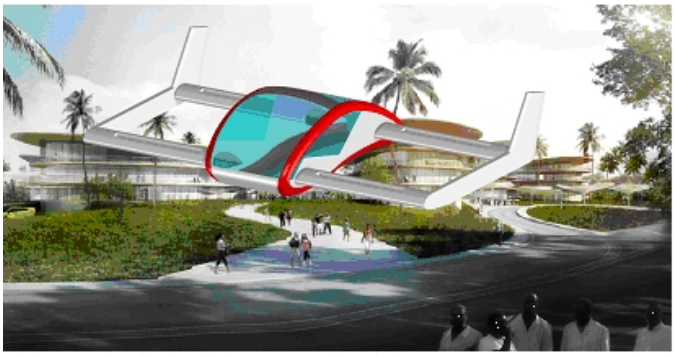

Figure 39. Another preliminary system rendering

Energy consumption and GHG emissions of Blowing urban-craft has been estimated assuming CFD results and verified according to the well-known second principle based EMIPS Method [19, 20] as modified by Trancossi [18].

The evaluations consider a reference mission profile, which has been shown in Figure 40.

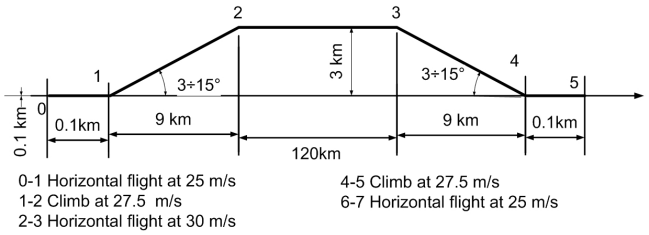

Figure 40. Reference mission profile.

The reference mission profile do not consider take off and landing operations to allow an effective comparison between aircraft of different nature including aircrafts and helicopters.

Table 1. Comparison against competitors

		Helicopter	Helicopter	Aircraft	Aircraft	Aircraft	Hybrid
Parameters		CH7 Compress	Siton AH 130	Rans S19 Venterra	Pipistrel Sinus	Pipistrel WHATsUP	BlowWing UrbanCraft
Crew	N.	1	1	1	1		1
Passengers	N.	1	1	1	1		1
Dimensions	m x m	7.5 x 6.2	8.9 x 7.7	6 x 8	6.6 x 15	6.5 x 10.5	5.5 x 6
Empty Weight	Kg	275	290	372	284	314	320
Max Fuel	Litres	60	90	91	60	-	-
MTOW	Kg	450	590	599	544	550	600
Cruise Speed	kn	99	92	110	110	121	110
Max range	mi	298	373	580	>700	150	250
Service ceiling	m	5000	5000	4500	8800	4877	3200
Rate of climb		8	8.5	4.6	6.2	6.1	7
Motorization	-	Rotax 914	Solar T62 Turboshaft	Rotax 912ULS	Rotax 912UL	Siemens Electric	Plettemberg elec. 20 units
Power	kW	84.5	97	60	150	50	3 kW
Fuel	-	Unleaded	Jet A-1	Unleaded	PV	electric	electric
Fuel cons.	litres/100km	12.5	13	9	6	-	
GHG Emissions	kg/100 km	27.5	28.5	22.5	15	4.2*	3.6*

The results clearly show the excellent energy efficiency and low emissions of the vehicle with respect to the competitors in a speed regime between 25 and 30 m/s. Encouraging results have been obtained, even if they are still a preliminary evaluation assessed on the basis an approximated but well tested method that needs to be evaluated with a more effective method.

References

1. Trancossi, M., “An Overview Of Scientific And Technical Literature On Coandă Effect Applied To Nozzles”, SAE Technical Papers N. 2011-01-2591, Issn 0148-7191, 2011. doi:
2. Drăgan, V., “Contributions regarding the design of a self super circulated rotary wing,” ModTech International Conference, 2012.
3. Trancossi, M., Stewart, J., & Pascoa, J. C., “A New Propelled Wing Aircraft Configuration.” ASME 2016 International Mechanical Engineering Congress and Exposition. American Society of Mechanical Engineers, 2016. p. V001T03A048-V001T03A048. doi:10.1115/IMECE2016-65373.
4. Rosero, J. A., et al. "Moving towards a more electric aircraft." IEEE Aerospace and Electronic Systems Magazine 22.3, 2007, pp. 3-9. doi: 10.1109/MAES.2007.340500.
5. Cao, Wenping, et al. "Overview of electric motor technologies used for more electric aircraft (MEA)." IEEE Transactions on Industrial Electronics 59.9, 2012, pp. 3523-3531. doi: 10.1109/TIE.2011.2165453.
6. Boglietti, Aldo, et al. "The safety critical electric machines and drives in the more electric aircraft: A survey." Industrial Electronics, 2009. IECON'09. 35th Annual Conference of IEEE. IEEE, 2009. doi: 10.1109/IECON.2009.5415238.
7. Young, K., Wang, C., Wang, L. Y., & Strunz, K., “2013, Electric vehicle battery technologies.” In Electric Vehicle Integration into Modern Power Networks (pp. 15-56). Springer New York.
8. Kiwan A R. “Helicopter performance evaluation (HELPE) computer model,” AD Report AD-A284 319/1, 1994.
9. Wood T L, Livingston C L, “An energy method for prediction of helicopter manoeuvrability”, AD Report, ADA021266, 1971.
10. Phillis, Y. A. and Venkatesan C., “Fundamentals of Helicopter Dynamics," Journal of Intelligent & Robotic Systems 83.1, 2016; 161-162. doi:10.1007/s10846-016-0337-0.
11. Ameyugo,0 G, Taylor M and Singh, R., “Distributed propulsion feasibility studies.” 25th International Congress of the Aeronautical Sciences, 2006. http://www.icas.org/ICAS_ARCHIVE/ICAS2006/PAPERS/250.PDF
12. Godard, J L. “Semi-buried engine installation: The NACRE project experience.” 27th International Congress of the Aeronautical Sciences (ICAS), 2010. http://www.icas.org/ICAS_ARCHIVE/ICAS2010/PAPERS/123.PDF
13. Ueda, T. and Dowell, E.H., A new solution method for lifting surfaces in subsonic flow. AIAA Journal, 20(3), 1982, pp.348-355. doi: 10.2514/3.7916.
14. Findanis, N. and Ahmed, N.A., “Flow studies of a forward swept wing fitted with active flow control.” Advances and Applications in Fluid Mechanics, 15(2), p.163. http://search.proquest.com/openview/0e50c149a96d15732de0be1fa63a5520/1?pq-origsite=gscholar&cbl=1816358
15. Kurtulus, D.F., David, L., Farcy, A. and Alemdaroglu, N., 2008. Aerodynamic characteristics of flapping motion in hover. Experiments in Fluids, 44(1), pp.23-36. doi:10.1007/s00348-007-0369-0.
16. Kiwan A R. “Helicopter performance evaluation (HELPE) computer model,” AD Report AD-A284 319/1, 1994.
17. Wood T L, Livingston C L, An energy method for prediction of helicopter manoeuvrability AD Report, ADA021266, 1971.
18. Trancossi, M., "What price of speed? A critical revision through constructal optimization of transport modes." International Journal of Energy and Environmental Engineering 7.4, 2016, pp.425-448. doi:10.1007/s40095-015-0160-6
19. Dewulf, J., & Van Langenhove, H., “Exergetic material input per unit of service (EMIPS) for the assessment of resource productivity of transport commodities. Resources, Conservation and Recycling,” 38(2), 2003, pp. 161-174. doi: /10.1016/S0921-3449(02)00152-0
20. Seckin, C., Sciubba, E. and Bayulken, A.R., “Extended exergy analysis of Turkish transportation sector.” Journal of Cleaner Production, 47, 2013, pp.422-436. doi: 10.1016/j.jclepro.2012.07.008.
21. Trancossi, M., "A response to industrial maturity and energetic issues: a possible solution based on constructal law." European Transport Research Review 7, no. 1 (2015): 1-14. doi:10.1007/s12544-014-0150-4.
22. Nasiri, M. and Rezazade, M., "Simulation and Visualization Environment for Nonlinear Helicopter Flight Dynamics," SAE Technical Paper 2006-01-2425, 2006, doi:10.4271/2006-01-2425.
23. Phillis, Y.A., and C. Venkatesan, Fundamentals of Helicopter Dynamics. Journal of Intelligent & Robotic Systems, 83(1), 2016, pp.161-162. doi: 10.1007/s10846-016-0337-0.

24. Hardier, G., Seren, C., and Ezerzere, P., "On-line Estimation of Longitudinal Flight Parameters," SAE Technical Paper 2011-01-2769, 2011, doi:10.4271/2011-01-2769.
25. Trancossi, M., Dumas, A., Madonia, M., Subhash, M. et al., "Preliminary Implementation Study of ACHEON Thrust and Vector Electrical Propulsion on a STOL Light Utility Aircraft," SAE Technical Paper 2015-01-2422, 2015, doi:10.4271/2015-01-2422.
26. Zhuang N., Xiang J., Luo Z., and Ren Y., "Calculation of helicopter maneuverability in forward flight based on energy method", Computer Modelling & New Technologies, 18(5), pp. 50-54, 2014. http://www.cmnt.lv/en/on-line-journal/2014/2014-volume-18-5/1160-mathematical-and-computer-modelling/calculation-of-helicopter-maneuverability-in-forward-flight-based-on-energy-method
27. Johnson, W., Lau, B.H. and Bowles, J.V., Calculated performance, stability, and maneuverability of high speed tilting proprotor aircraft. NASA Technical Memorandum 88349, 1987. https://ntrs.nasa.gov/archive/nasa/casi.ntrs.nasa.gov/19870008262.pdf
28. Tai, T.C., "Simulation and analysis of V-22 tiltrotor aircraft forward-flight flowfield." Journal of aircraft, 33(2), pp.369-376, 1996. doi: 10.2514/3.46947.
29. Boeing Commercial Airplane Group et al., "Civil tiltrotor Missions and Applications Phase II: The Commercial Passenger Market," Prepared for National Aeronautics and Space Administration and Federal Aviation Administration, NASA CR 177576, 1991. https://ntrs.nasa.gov/archive/nasa/casi.ntrs.nasa.gov/19910016812.pdf
30. Whittle, R., "The Dream Machine: The Untold History of the Notorious V-22 Osprey", Simon and Schuster, pp.464, 2010;
31. Heyson, H. (1975). A momentum analysis of helicopters and autogyros in inclined descent. NASA-TN-D-7917
32. Glauert, H., "The theory of the autogyro." Journal of the Royal Aeronautical Society, 31(198), 1927, pp.483-508. http://naca.central.cranfield.ac.uk/reports/arc/rm/1111.pdf
33. Houston, S. and Thomson, D., "On the modelling of gyroplane flight dynamics." Progress in Aerospace Sciences, 88, 2016, pp. 43-58. doi: 10.1016/j.paerosci.2016.11.001.
34. Gibbings, D., "The Fairey Rotodyne—technology before its time?." The Aeronautical Journal 108.1089, 2004, pp.565-574. doi: 10.1017/S0001924000000397
35. Massey H., "Means and method for increasing the magnus effect", Pat. US2344515 A, 1941.
36. Coandă H., "Jet Propelled Aircraft", Pat. US2946540 A, 1948.
37. Goembel P., "Jet propelled airplane with wing discharge slot", Pat. US2479487, 1946.
38. Bradbury D., and Meyer C., "Wing-mounted jet-propulsion system with controllable discharge outlet", Pat. US2420323 A, 1943.
39. Capuani, A., "Aircraft with jet propulsion." U.S. Patent 4,478,378, 1984.
40. Capuani, A., "Jet-propelled aircraft." U.S. Patent 4,969,614, 1990.
41. Trancossi, M., "An Overview of Scientific and Technical Literature on Coandă Effect Applied to Nozzles," SAE Technical Paper 2011-01-2591, 2011, doi:10.4271/2011-01-2591.
42. Trancossi, M. and Dumas, A., "A.C.H.E.O.N.: Aerial Coandă High Efficiency Orienting-jet Nozzle," SAE Technical Paper 2011-01-2737, 2011, doi:10.4271/2011-01-2737.
43. Páscoa, J.C., Brójo F. M. P., and Monteiro J. M. M., "Numerical Simulation of Magneto-plasma Thrusters for Aerospace Propulsion Using and MHD Formulation," Paper O-7.2, Proc. 14th International Conference on Emerging Nuclear Energy Systems, Instituto Tecnológico e Nuclear, 6 pgs, 2009.
44. Abdollahzadeh, M., et al., P.J., "Numerical design and analysis of a multi-DBD actuator configuration for the experimental testing of ACHEON nozzle model," Aerospace Science and Technology, 41, 2015. pp.259-273. doi: 10.1016/j.ast.2014.12.012
45. Trancossi, M., Stewart, J., Maharshi, S. and Angeli, D., "Mathematical model of a constructal Coandă effect nozzle." Journal of Applied Fluid Mechanics, 9(6), pp.2813-2822, 2016. http://jafmonline.net/JournalArchive/download?file_ID=41384&issue_ID=237
46. Trancossi, M., "Design of ACHEON Thrust and Vector Propulsion System," SAE Technical Paper 2015-01-2425, 2015, doi:10.4271/2015-01-2425.
47. Trancossi, M. et al. "Preliminary implementation study of ACHEON thrust and vector electrical propulsion on a STOL light utility aircraft," SAE Technical Paper No. 2015-01-2422, 2015.
48. Trancossi, M., Dumas, A., Madonia, M., Subhash, M. et al., "Preliminary Implementation Study of ACHEON Thrust and Vector Electrical Propulsion on a STOL Light Utility Aircraft," SAE Technical Paper 2015-01-2422, 2015, doi:10.4271/2015-01-2422.
49. Nelson, C. P. "Integrated and/or modular high-speed aircraft." U.S. Patent No. 6,938,854, 2005.
50. Radespiel, R., Burnazzi, M., Casper, M. and Scholz, P., "Active flow control for high lift with steady blowing," The Aeronautical Journal, 120(1223), 2016, pp.171-200. doi: 10.1017/aer.2015.7.
51. Landa, T., Radespiel, R., and Wild, J., "Numerical simulations of stream wise vortices on a generic high-lift configuration. In54th AIAA Aerospace Sciences Meeting 2016 (p. 0304). doi: 10.2514/6.2016-0304.
52. Drăgan V. "A new mathematical model for high thickness Coandă effect wall jets," Review of the Air Force Academy. 2013. http://www.afahc.ro/ro/revista/Nr_1_2013/14%20Valeriu%20Dragan.pdf
53. Roderick, W. E. B., "Use of the Coandă Effect for the Deflection of Jet Sheets of a Smoothly Curve Surfaces, Part II", University of Toronto, Institute of Aerophysics, Technical Note No.5, 1961.
54. Benner, S.D., "The Coandă effect at deflection surfaces widely separated from the jet nozzle" University of Toronto. UTISA Technical Note no. 78, 1965.
55. Drăgan, V., "Contributions regarding the design of a self super circulated rotary wing," ModTech International Conference, 2012.
56. Stoll A.M., "Comparison of CFD and Experimental Results of the LEAPTech Distributed Electric Propulsion Blown Wing." 15th AIAA Aviation Technology, Integration, and Operations Conference 2015 (p. 3188), 2015. doi: 10.2514/6.2015-3188
57. Dubois, A., et al., "Design of an Electric Propulsion System for SCEPTOR," 16th AIAA Aviation Technology, Integration, and Operations Conference, AIAA, Washington, D.C., June 2016. doi: 10.2514/6.2016-3925.
58. Clarke S., Papathakis K., Samuel A., Lin Y., and Ginn S., "NASA SCEPTOR electric concept aircraft power system: X-plane electric propulsion system design and qualification for crewed flight testing." Transportation Electrification Conference and Expo (ITEC), 2016 IEEE 2016 Jun 27 (pp. 1-27). IEEE, 2016. doi: 10.1109/ITEC.2016.7520287.
59. Casey M, Wintergerste T. ERCOFTAC Special Interest Group on "Quality and Trust in Industrial CFD" Best Practice

Guidelines. Version 1.0; January 2000. http://server2.docfoc.com/uploads/Z2015/12/04/fVL0J3svWG/b91e04a4955154b8971b78afd8ffe65f.pdf
60. Rizzi, A., and Vos, J., "Towards Establishing Credibility in Computational Fluid Dynamics." AIAA Journal 1998; 36(5), 1998, pp. 668-675. doi: 10.2514/2.442.
61. Celik I., Li J., Hu G., Shaffer C., "Limitations of Richardson Extrapolation and Some Possible Remedies" J Fluids Eng, 127 (2005), pp. 795-805. doi:10.1115/1.1949646.
62. Schlichting, H., Gersten, K., Krause, E. and Oertel, H., Boundary-layer theory (Vol. 7). New York: McGraw-hill, 1960. ISBN: 978-3-662-52917-1
63. Pfingsten, K.C. and Radespiel, R., "Numerical simulation of a wing with a gapless high-lift system using circulation control." New Results in Numerical and Experimental Fluid Mechanics VI, 2008, pp.71-79. doi: 10.1007/978-3-540-74460-3_9.
64. Besagni, G., Mereu, R., Chiesa, P. and Inzoli, F., "An Integrated Lumped Parameter-CFD approach for off-design ejector performance evaluation." Energy Conversion and Management, 105, 2015. pp.697-715. doi: 10.1016/j.enconman.2015.08.029.
65. Spalart, P. and Allmaras, S., "A one-equation turbulence model for aerodynamic flows." In 30th aerospace sciences meeting and exhibit, 1992, p. 439. doi: 10.2514/6.1992-439.
66. Spalart, P.R. and Shur, M., "On the sensitization of turbulence models to rotation and curvature." Aerospace Science and Technology, 1(5), 1998. pp.297-302. doi: 10.1016/S1270-9638(97)90051-1
67. Wilcox, D.A., "Simulation of transition with a two-equation turbulence model." AIAA journal, 32(2), 1994, pp.247-255. doi: 10.2514/3.59994.
68. Wilcox, D.C., "Formulation of the kΩ turbulence model revisited." AIAA journal, 46(11), 2008.pp.2823-2838. doi: 10.2514/1.36541
69. Kim, J. Y., Ghajar, A. J., Tang, C., & Foutch, G. L. "Comparison of near-wall treatment methods for high Reynolds number backward-facing step flow. International Journal of Computational Fluid Dynamics, 19(7), 2005, pp. 493-500. doi: 10.1080/10618560500502519.
70. Jang DS, Jetli R, and Acharya S. "Comparision of the PISO, SIMPLER and SIMPLEC Algorithms for the treatment of the Pressure-Velocity Coupling in Steady Flow Problems." Num Heat Transf 1986; 10(3), 1986, 209-228. doi: 10.1080/10407788608913517
71. Ghaneeizad, S.M., Karamigolbaghi, M., Atkinson, J.F. and Bennett, S.J., 2016. "Evaluation of turbulence closure models for the simulation of circular impinging jets." In River Flow 2016, CRC Press, 2016, pp. 122-129. doi: 10.1201/9781315644479-23
72. http://aeromobil.com/
73. www.urbanaero.com/category/x-hawk
74. VV.AA. (2002). Skycar gets new engines as Moller hires help with certification work, FLIGHT INTERNATIONAL, 31 Dec. 2002
75. http://moller.com/
76. https://www.xplorair.com/
77. https://www.terrafugia.com/tf-x/
78. http://www.macroindustries.com/website/files/skyrider/1024_/index_main.htm
79. Young, K., Wang, C., Wang, L. Y., & Strunz, K. (2013). Electric vehicle battery technologies. In Electric Vehicle Integration into Modern Power Networks (pp. 15-56). Springer New York.
80. Hussain, M., "Prototyping and testing of an Innovative EDF propelled UAV with VTOL and STOL capability," Final year project, BSc Aeronautical Engineering, Sheffield Hallam University, supervisor Trancossi M., 2017.
81. Hussain, M. and Trancossi M., "A new VTOL propelled wing for flying cars: preliminary design and CFD analysis", SAE Aerotech 2017, Paper n. 17ATC-0039.

Definitions/Abbreviations

EDF	electric ducted fan
Ω	angular speed (rpm, rad/s)
δ	distance of the rear ailerons from center of mass (m)
δ_a	boundary layer thickness
δ_b	stream
ε	thrust angle (deg, rad)
γ	glide angle (deg, rad)
ϕ	pitch angle of helicopter propeller (deg, rad)
ρ	density (kg/m^3)
τ	Shear stress (kg/m^2)
A	area (m^2)
D	drag (N)
I	moment of inertia (kg m^2)
L	lift (N)
R	radius of Coandă surface (m)
T	thrust (N)
W	weight
h	Coandă jet thiickness
n	number of propeller
p	pressure (Pa)
u	velocity (m/s)

Contact Information

Dr. Michele Trancossi
Senior Lecturer
Sheffield Hallam University
m.trancossi@shu.ac.uk; m.trancossi@gmail.com